FAST-CONVERGENCE SINGULAR VALUE DECOMPOSITION FOR TRACKING TIME-VARYING CHANNELS IN MASSIVE MIMO SYSTEMS

Pei-Yun Tsai, Yi Chang, and Jian-Lin Li

Department of Electrical Engineering, National Central University, Taoyuan, Taiwan

ABSTRACT

A fast-convergence singular value decomposition (SVD) algorithm is developed for tracking time-varying channels in massive MIMO precoding/beamforming systems. Since only strong eigen-modes are selected for data transmission in these systems, our SVD algorithm exploits the properties of partial decomposition and temporal correlation. Besides, the proposed self-adjusting inverse power method can achieve fast convergence by modifying the shift according to the intermediate result during each iteration. Furthermore, the singular vectors and values of the desired eigen-modes can be computed simultaneously. Thus, parallel processing is possible to facilitate high-throughput implementation. Compared to the self-power method with super linear convergence, the self-adjusting inverse power method has better convergence and lower complexity. Good channel tracking capability is also demonstrated.

***Index Terms* —** Massive MIMO, SVD, channel tracking, inverse power method.

1. INTRODUCTION

Singular value decomposition plays an important role in multiple-input multiple-output (MIMO) wireless communication systems. It can generate precoding/beamforming and decoding matrix at the transmitter and receiver side to transform the spatial channel into parallel subchannels [1]. User data then can be transmitted through these spatial subchannels with stronger channel gains. In other words, singular value decomposition helps to realize signal concentration and interference removal. Thus, its applications in MIMO systems are widely seen.

For an $N \times N$ matrix, the complexity of SVD is usually described by $\mathcal{O}(N^3)$. In [2], the Jacobi algorithm is adopted, which uses a series of Jacobi rotations to nullify the off-diagonal terms and to generate singular values as well as singular vectors for the channel matrix of size $2 \times 2 \sim 8 \times 8$. In [3][4], two-step algorithms containing bidiagonalization and iterative diagonalization are employed for 4×4 or 8×8 MIMO systems. The self-power method is employed in [5] for 4×4 channel matrixes. As the number of antennas at the base station becomes large, known as the massive MIMO technique for the upcoming 5G systems, the computation complexity grows rapidly and may be unaffordable for real-time implementation if the conventional schemes are adopted. Consequently, more properties of the SVD for massive MIMO precoding applications should be exploited. Iterative approaches are often involved for SVD. Both [5] and [6] emphasize the importance of accelerating convergence to save the computation. In [6], channel temporal correlation is utilized and the recursive algorithm is derived to reduce the complexity. In addition, for the massive MIMO systems, only parts of the singular vectors corresponding to the strong eigen-modes are desired. Thus, solving all the singular vectors are not necessary [6][7]. In light of the above, partial decomposition, fast convergence, and temporal correlation are essential properties that must be taken into consideration when we develop the SVD algorithm for massive MIMO systems.

In this paper, we present the SVD algorithm for tackling time-varying channel matrix in massive MIMO systems. The QuaDriGa and 3GPP three-dimensional channel model is adopted so as to examine channel properties in massive MIMO systems [8][9]. A hybrid power method is then adopted, which combines self-power method (SPM) [5] and self-adjusting inverse power method (SA-IPM). The SPM is employed in the initialization phase to compute only the desired singular values and the corresponding singular vectors, which can be regarded as the first acquisition. The proposed SA-IPM then follows in the tracking phase for subsequent tuning. Although the channel response and its singular values are time-varying, we can take advantage of their temporal correlation. Consequently, the previous singular-value information is reused as the shift in the SA-IPM to obtain the latest SVD result and to shorten the convergence time. Furthermore, the SA-IPM is advantageous in the following two aspects. On one hand, the shift is adjusted during each iteration so as to upgrade convergence. On the other hand, the singular vectors can be computed in parallel. Thus, high-throughput real-time processing becomes feasible. The performance simulation results demonstrate its excellent tracking capability. The complexity is also evaluated to show the saving attained by the proposed method.

In the following, the system model and channel model are first illustrated in Sec. 2. The proposed SVD algorithm for time-varying channel matrix is given in Sec. 3. The complexity analysis and performance simulation are shown in Sec. 4. Finally, Sec. 5 gives a brief conclusion.

2. SYSTEM MODEL AND CHANNEL MODEL

In massive MIMO precoding systems with N receive antennas and M transmit antennas, the received signal $\mathbf{y} \in \mathbb{C}^{N\times 1}$ can be expressed as

$$\mathbf{y} = \mathbf{HFx} + \mathbf{n} \tag{1}$$

where $\mathbf{x} \in \mathbb{C}^{S\times 1}$ is the transmitted signal vector with S streams; $\mathbf{H} \in \mathbb{C}^{N\times M}$ is the channel response; $\mathbf{n}$ is the noise vector. By SVD, $\mathbf{H} = \bar{\mathbf{U}}\bar{\mathbf{\Sigma}}\bar{\mathbf{V}}^{\mathrm{H}}$, where $\bar{\mathbf{U}} \in \mathbb{C}^{N\times N}$ and $\bar{\mathbf{V}} \in \mathbb{C}^{M\times M}$ are the left singular matrix and the right singular matrix, respectively; $\bar{\mathbf{\Sigma}} \in \mathbb{R}^{N\times M}$ is a real diagonal matrix with singular values on its diagonal. Usually $N \ll M$ in the downlink. Given precoding matrix $\mathbf{F} = \mathbf{V} \in \mathbb{C}^{M\times S}$, which consists of S right singular vectors in $\bar{\mathbf{V}}$ corresponding to the S strongest singular values. With decoding matrix $\mathbf{U}^{\mathrm{H}} \in \mathbb{C}^{S\times N}$, the stronger channel eigen-modes then are used to transmit S streams, and thus we have

$$\mathbf{z} = \mathbf{U}^{\mathrm{H}}\mathbf{y} = \mathbf{U}^{\mathrm{H}}\mathbf{HVx} + \mathbf{U}^{\mathrm{H}}\mathbf{n} = \mathbf{\Sigma x} + \mathbf{U}^{\mathrm{H}}\mathbf{n}. \tag{2}$$

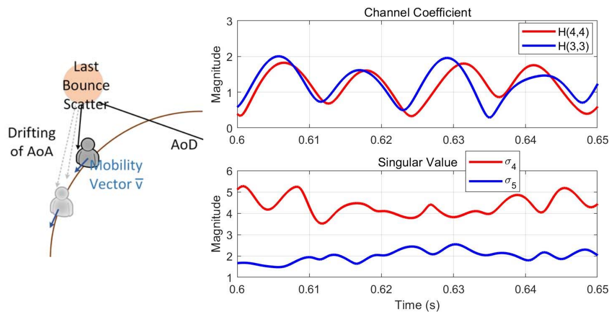

Fig. 1 Time-varying angle of arrival and singular values along a circular trajectory.

To model the three-dimensional (3D) spatial channel characteristics for massive MIMO systems, the (n_r, n_t) th coefficient of the channel matrix takes the form of [9]

$$\mathbf{H}_m(n_r, n_t) = \sum_{l=1}^{L} \sqrt{\frac{P_l}{U}} \sum_{u=1}^{U} \exp(jk\hat{\mathbf{r}}_{rx,l,u}^T[\mathrm{m}]\bar{\mathbf{d}}_{rx,n_r}) \exp(jk\hat{\mathbf{r}}_{tx,l,u}^T[\mathrm{m}]\bar{\mathbf{d}}_{tx,n_t})\exp(jk\hat{\mathbf{r}}_{rx,l,u}^T[m]\bar{\mathbf{v}}mT_s) \quad (3)$$

where P_l denotes the path power of cluster l; $k = 2\pi/\lambda$; T_s is the sampling period. $\hat{\mathbf{r}}_{tx,l,u}^T[\mathrm{m}]$ ($\hat{\mathbf{r}}_{rx,l,u}^T[\mathrm{m}]$) is the spherical unit vector with azimuth departure (arrival) angle $\phi_{l,u}^{tx}[m]$ ($\phi_{l,u}^{rx}[m]$) and elevation departure (arrival) angle $\theta_{l,u}^{tx}[m]$ ($\theta_{l,u}^{rx}[m]$) of the lth cluster and the uth subpath at time index m,

$$\hat{\mathbf{r}}_{tx,l,u}[\mathrm{m}] = \begin{bmatrix} sin(\theta_{l,u}^{tx}[m])\cos(\phi_{l,u}^{tx}[m]) \\ sin(\theta_{l,u}^{tx}[m])\sin(\phi_{l,u}^{tx}[m]) \\ cos(\theta_{l,u}^{tx}[m]) \end{bmatrix}. \quad (4)$$

According to the K factor, $P_1 = K\sum_{l=2}^{L} P_l$ and $\sum_{l=1}^{L} P_l = 1$. The uniform planar array (UPA) is considered because smaller antenna array dimensions are allowed for massive MIMO systems and it supports beamforming in elevation [10]. The antenna element inside the array is represented by the location vector $\bar{\mathbf{d}}_{tx,n_t}$ ($\bar{\mathbf{d}}_{rx,n_r}$) at the transmitter (receiver) side. The movement of the mobile station is described by the mobility vector $\bar{\mathbf{v}}$ with travel azimuth angle, elevation angle and speed $|\bar{\mathbf{v}}|$.

To describe time-evolving sequence of channel coefficients $\mathbf{H}_m$ along the user trajectory, the birth and death of scattering clusters are introduced in [8]. The trajectory is partitioned into several segments. For each segment, the parameters remain unchanged. Smooth transition in the overlapping region between two adjacent segments is achieved by the ramp with a squared sine function,

$$R(m_{overlap}) = \sin^2\left(\frac{\pi}{2}\frac{m_{overlap}}{O}\right), \quad (5)$$

where O is the index duration for the overlapping region and $-O \leq m_{overlap} \leq O$. Thus, the power of old clusters ramps down and the power of new clusters ramp up. Given that a user moves along a circular trajectory with a radius of 100m and the antenna spacing in the antenna array is half-wavelength, Fig. 1 depicts the time-varying channel coefficients and singular values of 9×64 channel matrix $\mathbf{H}_m$ with 12 clusters each having 10 subpaths. Assume that the mobility is 3Km/hr and the maximum Doppler frequency is 83.3Hz. Each segment is about 22m and the overlapping region has a length of 11m. The drifting effect is incorporated to update the snapshot of azimuth and elevation arrival angle according to position of the mobile station along the trajectory inside each segment [8]. The azimuth and elevation departure angles keep fixed [8][11].

Algorithm 1: Hybrid Power Method

Input: $\mathbf{H}_m$
Output: $\mathbf{U}_m$, $\mathbf{\Sigma}_m$, $\mathbf{V}_m$
1: $\mathbf{A}_m = \mathbf{H}_m \cdot \mathbf{H}_m^H$
2: **if (Initialization)** // Initialization phase
3: $[\mathbf{V}_m] = \mathrm{SPM}(\mathbf{A}_m, I_1)$ // Self-Power method
4: **else** // Tracking phase
5: **for** $r = 1$ *to* S
6: $\beta_r^{(0)} = (\mathbf{\Sigma}_{m-\Delta}(r,r))^2$, $\bar{\mathbf{q}}_r^{(0)} = \mathbf{V}_{m-\Delta}(:,r)$
7: $\left[\bar{\mathbf{q}}_r^{(I_2)}, \beta_r^{(I_2)}\right] = \text{SA-IPM}\left(\left(\mathbf{A}_m - \left(\beta_r^{(0)} \cdot \mathbf{I}\right)\right), \bar{\mathbf{q}}_r^{(0)}\right)$
8: **end**
9: $\mathbf{V}_m = [\bar{\mathbf{q}}_1^{(I_2)} \quad \bar{\mathbf{q}}_2^{(I_2)} \quad \dots \quad \bar{\mathbf{q}}_S^{(I_2)}]$
10: **endif**
11: $\mathbf{T}_m = \mathbf{H}_m^H \mathbf{V}_m$
12: **for** $r = 1$ *to* S
13: $\mathbf{\Sigma}_m(r,r) = \|\mathbf{T}_m(:,r)\|$
14: $\mathbf{U}_m(:,r) = \mathbf{T}_m(:,r)/\mathbf{\Sigma}_m(r,r)$
15: **end**

3. PROPOSED SVD TRACKING ALGORITHM

To develop SVD algorithm for tracking time-varying channel in massive MIMO systems, the following properties must be exploited.

- Only the desired singular vectors corresponding to strong singular values are computed for complexity reduction.
- Fast convergence is necessary to facilitate channel tracking and to save computation time.
- Correlation of channel response must be utilized in order to accelerate convergence or to reduce complexity.

We then use the hybrid power method for SVD, provided in Algorithm 1, to track channel variation. Initially, the channel usable eigen-modes are unknown, and thus search for strong singular values is necessary. The self-power method (SPM) which has a super linear convergence rate [5] is utilized in the first acquisition phase. The eigenvalues together with eigenvectors of $\mathbf{A}_m$, namely singular values and associated left singular vectors of $\mathbf{H}_m$, are computed sequentially from the one with the largest magnitude, as described in Algorithm 2. Assume that S singular vectors are required, which can be determined either by the number of streams to be transmitted or by the selected eigen-modes according to the magnitude of singular values. For each vector, I_1 iterations are executed. When the rth singular vector is obtained, the deflation operation is performed as in Step 7 of Algorithm 2 to remove the contribution of that vector in the matrix to be decomposed.

In the tracking phase, the SA-IPM is adopted to accelerate the convergence. The QR decomposition (QRD) is adopted to solve the inverse operation as described in Algorithm 3. The QRD can handle the rank-deficient matrix. Hence, when the shift is equal to the eigenvalue, the eigenvector can be obtained immediately from the vector spanning the null space as given in Step 4, where ϵ is a tiny value. Moreover, based on the concept of Rayleigh quotient iteration [12], the shift is adjusted according to the information during each iteration so as to approach the eigenvalues very quickly. The explanation is given in the following.

From step 2 and step 8 in Algorithm 3 for $i = i_2 - 1$, the SA-IPM calculates

$$\mathbf{z}_r^{(i+1)} = \left(\mathbf{A} - \left(\beta_r^{(i)} \cdot \mathbf{I}\right)\right)^{-1} \bar{\mathbf{q}}_r^{(i)} = \mathbf{B}^{(i)}\bar{\mathbf{q}}_r^{(i)}, \quad (6)$$

Algorithm 2: SPM [5]

```
Function SPM(A, I_1)
Output: V
A_1^(0) = A,
for r = 1 to S
    for i_1 = 1,2,...,I_1
        A_r^(i_1) = k_r^(i-1) A_r^(i_1-1) A_r^(i_1-1)
    end
    v_r = A_r^(I_1)(:,1) / ||A_r^(I_1)(:,1)||
    A_(r+1)^(0) = (I - v_r v_r^H) A_r^(0)
end
V = [v_1  v_2  ...  v_S]
```

Algorithm 3: SA-IPM

```
Function SA-IPM((A - (β^(0)·I)), q̄^(0))
Output: q̄^(I_2), β^(I_2)
for i_2 = 1,2,...,I_2
    [Q^(i_2), R^(i_2)] = qr(A - (β^(i_2-1)·I))
    if (|R^(i_2)(N,N)| < ϵ)
        q̄^(I_2) = Q^(i_2)(:,N)
        β^(I_2) = β^(i_2-1)
        break;
    else
        z^(i_2) = (R^(i_2))^(-1) Q^(i_2)H q̄^(i_2-1)
        if (sign(real(q̄_r^(i)H z_r^(i+1))) > 0)
            β^(I_2) = β^(i_2-1) + 1/||z^(i_2)||
        else
            β^(I_2) = β^(i_2-1) - 1/||z^(i_2)||
        endif
        q̄^(I_2) = z^(i_2)/||z^(i_2)||
    endif
end
```

for the rth vector. Without loss of generality, subscript m is dropped here. By QR decomposition,

$$\left(\mathbf{B}^{(i)}\right)^{-1} = \left(\mathbf{A} - \left(\beta_r^{(i)} \cdot \mathbf{I}\right)\right) = \mathbf{Q}^{(i+1)}\mathbf{R}^{(i+1)}, \tag{7}$$

where $\mathbf{Q}^{(i+1)}$ and $\mathbf{R}^{(i+1)}$ are unitary and upper triangular matrixes.

Assume that $\mathbf{A}$ has at least N linearly independent eigenvectors $\mathbf{q}_r$ and associated eigenvalues $\lambda_r = \beta_r^{(i)} + \delta_r^{(i)}$ for $1 \le r \le N$. Thus, matrix $\mathbf{B}^{(i)}$ has an eigenpair $\frac{1}{\delta_r^{(i)}} \gg 1$ and $\mathbf{q}_r$. If $\beta_r^{(i)}$ equals the eigenvalue, namely $\delta_r^{(i)} = 0$, then inverse of $\left(\mathbf{A} - \left(\beta_r^{(i)} \cdot \mathbf{I}\right)\right)$ is infeasible. However, due to the rank deficiency,

$$\mathbf{R}^{(i+1)}(N,N) = 0 \tag{8}$$

and

$$\mathbf{Q}^{(i+1)}(:,N)^H \left(\mathbf{A} - \left(\beta_r^{(i)} \cdot \mathbf{I}\right)\right)^H = \mathbf{Q}^{(i+1)}(:,N)^H \left(\mathbf{A} - \left(\beta_r^{(i)} \cdot \mathbf{I}\right)\right) = \mathbf{0}_{1\times N}, \tag{9}$$

where the property that $\mathbf{A}$ is a Hermitian symmetric matrix is utilized. Thus, it is clear that

$$\left(\mathbf{A} - \left(\beta_r^{(i)} \cdot \mathbf{I}\right)\right)\mathbf{Q}^{(i+1)}(:,N) = \mathbf{0}_{N\times 1}. \tag{10}$$

Eq. (10) means that $\mathbf{Q}^{(i+1)}(:,N)$ lies in the null space of $\left(\mathbf{A} - \left(\beta_r^{(i)} \cdot \mathbf{I}\right)\right)$. Hence, it is the desired eigenvector.

On the other hand, if $\delta_r^{(i)} \neq 0$, let

$$\bar{\mathbf{q}}_r^{(i)} = \sum_{k=1}^{N} c_k^{(i)} \mathbf{q}_k. \tag{11}$$

Based on the first acquisition result from the SPM, $real(c_r^{(i)})$ is close to 1 and $\left|c_k^{(i)}\right|$ approaches 0 for $k \neq r$. Thus,

$$\mathbf{z}_r^{(i+1)} = \mathbf{B}^{(i)}\bar{\mathbf{q}}_r^{(i)} = \frac{1}{\delta_r^{(i)}} c_r^{(i)}\mathbf{q}_r + \sum_{k=1,k\neq r}^{N} c_k^{(i)} \left(\frac{1}{\lambda_k - \beta_r^{(i)}}\right)\mathbf{q}_k. \tag{12}$$

Given $\left|\lambda_r - \beta_r^{(i)}\right| = \left|\delta_r^{(i)}\right| \ll \left|\lambda_k - \beta_r^{(i)}\right|$ for $k \neq r$,

$$\left\|\mathbf{z}_r^{(i+1)}\right\| \approx \left|\frac{c_r^{(i)}}{\delta_r^{(i)}}\right| \approx \left|\frac{1}{\delta_r^{(i)}}\right|. \tag{13}$$

From Eq. (12), we can adjust the shift, $\beta_r^{(i)}$, to approach λ_r so as to accelerate the convergence if the sign of $\delta_r^{(i)}$ is known. Given that $\bar{\mathbf{q}}_r^{(i)H}\mathbf{q}_k = c_k^{(i)H}$ and $real(c_r^{(i)})$ close to 1, we can derive

$$\bar{\mathbf{q}}_r^{(i)H}\mathbf{z}_r^{(i+1)} = \frac{1}{\delta_r^{(i)}}\left|c_r^{(i)}\right|^2 + \sum_{k=1,k\neq r}^{N}\left|c_k^{(i)}\right|^2\left(\frac{1}{\lambda_k - \beta_r^{(i)}}\right). \tag{14}$$

Thus,

$$sign\left(real(\bar{\mathbf{q}}_r^{(i)H}\mathbf{z}_r^{(i+1)})\right) \cong sign\left(\frac{1}{\delta_r^{(i)}}\right) \tag{15}$$

because $\left|c_k^{(i)}\right|^2$ is small for $k \neq r$. From Eqs. (13) and (15), the shift can be adjusted in the following way. If $sign\left(real(\bar{\mathbf{q}}_r^{(i)H}\mathbf{z}_r^{(i+1)})\right) > 0$, $\beta_r^{(i+1)} = \beta_r^{(i)} + 1/\left\|\bar{\mathbf{z}}^{(i+1)}\right\|$ Otherwise, the adjustment can be made in the opposite direction and $\beta_r^{(i+1)} = \beta_r^{(i)} - 1/\left\|\bar{\mathbf{z}}^{(i+1)}\right\|$ to approach the eigenvalue. Note that the Rayleigh quotient iteration [12] uses the adjustment which can be given as follows

$$\bar{\mathbf{q}}_r^{(i)H}\left(\mathbf{A} - \left(\beta_r^{(i)} \cdot \mathbf{I}\right)\right)^{-1}\bar{\mathbf{q}}_r^{(i)} = \bar{\mathbf{q}}_r^{(i)H}\mathbf{z}_r^{(i+1)} \tag{16}$$

and its expression is shown in (14).

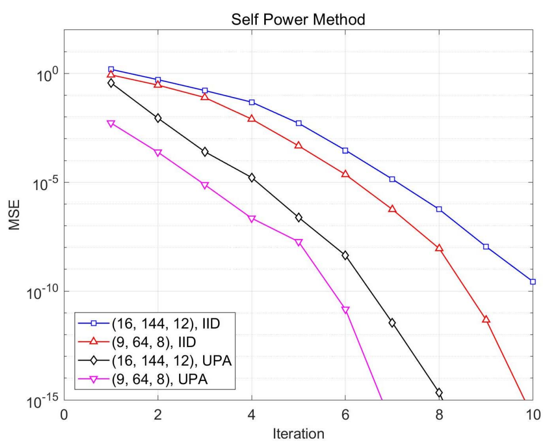

Fig. 2 Performance and convergence rate of the SPM in the first phase for different channel models.

3. PERFORMANCE SIMULATION AND COMPLEXITY ANALYSIS

The performance of the two-phase hybrid power method is given in Fig. 2 and Fig. 3. The antenna configuration and the number of spatial streams are denoted by (N, M, S). The K factor of the 3D channel model is 3dB in the simulation. The mean square error (MSE) of desired singular values, $\mathrm{E}\{|\sqrt{\lambda_r} - \mathbf{\Sigma}_m(r,r)|^2\}$, is evaluated. As depicted in Fig. 2, the self-power method shows different convergence rates for independent and identicallydistributed (IID) channel matrixes and the ones generated from UPA. It is clear that the spatial correlation makes the distribution of singular values different. In Fig. 3, the fast convergence rate of the SA-IPM is illustrated. Because the shift is adapted in each iteration, only few iterations are required. Compared to linear convergence of conventional inverse power method and super linear convergence of SPM, the proposed method has excellent convergence.

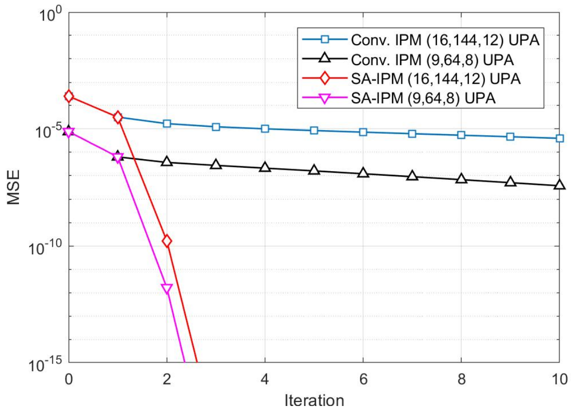

Fig. 3 Comparison of conventional inverse power method and the proposed SA-IPM.

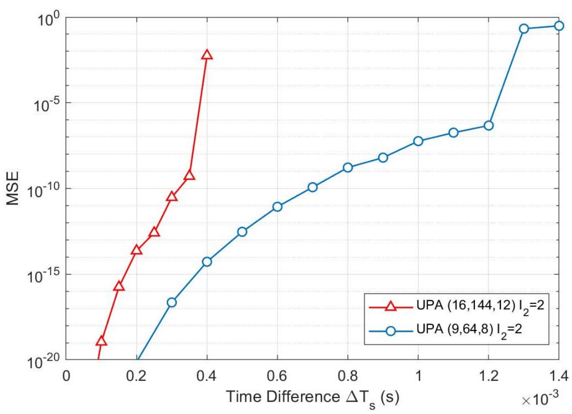

Fig. 4 Performance of SA-IPM in the tracking phase.

Once the desired singular values and singular vectors are acquired, the sequent tracking can simply rely on the SA-IPM. It can tolerate the time-variant singular value to a certain degree. Fig. 4 shows the MSE of the tracking result when Δ in step 6 of Algorithm 1 is set to various values given the maximum Doppler frequency 83.3Hz. The number of iterations is fixed and the sampling period (T_s) is 5μs. The antenna spacing is a half wavelength. Consequently, the SA-IPM can take advantage of channel temporal correlation and shows good tracking capability.

The complexity of the hybrid power method is evaluated and given in Table 1. From the table, we can see that the multiplication complexity overwhelms the remaining arithmetic computations. It is clear that a fast convergence rate brings not only the good tracking capability but also the linear complexity reduction. Furthermore, the complexity is sensitive to the matrix dimension of $\mathbf{A}_m$, but insensitive to the number of transmit antennas because parameter M exists in the non-iterative operations. Actually, we should always obtain the singular vectors of a small dimension at first if the channel matrix is not square. The SPM needs to deflate the matrix when a new singular vector is required. The deflation results in sequential computation for desired vectors and also computation-intensive. However, the proposed SA-IPM can adopt parallel processing because no dependency exists between r and r+1 in step 6 and 7 of Algorithm 1. This property is advantageous to the implementation either by GPU or dedicated hardware. Fig. 5 depicts the number of multiplications versus difference N and M values. The number of streams, S, is set to $3N/4$. The numbers of iterations I_1 and I_2 are selected to be 7 and 3, respectively. Compared to using the SPM with super linear convergence [5], switching to the SA-IPM for tracking channel variation can achieve reduced complexity as well as excellent tracking performance.

Table I: Complexity evaluation

	Add.	Mul.	Div.	Sqrt.
Non-iterative Operation (Algorithm 1)				
Step 1	$N^2(4M-2)$	$4N^2M$		
Step 11	$(4N-2)MS$	$4MNS$		
Step 13	$(2M-1)S$	$2MS$		S
Step 14			$2MS$	
Initialization Phase: Self-Power Method (Algorithm 2)				
Step 4	$N^2(4N-2)SI_1$	$4N^3SI_1$		
Step 6	$(2N-1)S$	$2NS$	$2NS$	S
Step 7	$(4N^3-2N^2+N)S$	$4N^2(N+1)S$		
Tracking Phase: Self-Adjusting Inverse Power Method				
Step 2	$(4N^3+N^2)SI_2$	$(4N^3+2N^2)SI_2$	$2N^2SI_2$	NSI_2
Step 8	$(6N^2-4N)SI_2$	$(6N^2-2N)SI_2$	$2NSI_2$	
Step 9	$(2N-1)SI_2$	$2NSI_2$		
Step 10/12	$2NSI_2$	$2NSI_2$	SI_2	SI_2
Step 14		$2NSI_2$		

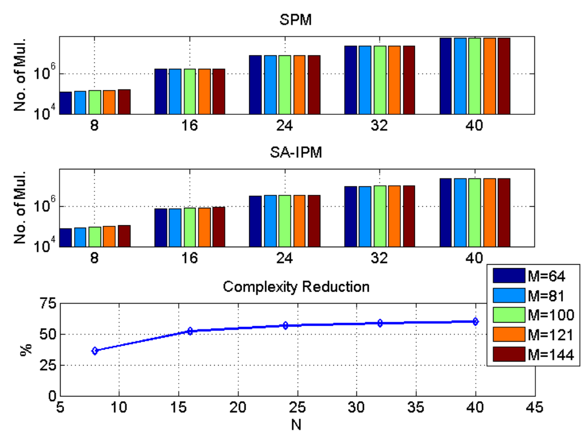

Fig. 5 Complexity comparison.

5. CONCLUSION

A singular value decomposition method is developed for channel tracking in the massive MIMO systems. The SA-IPM can adjust the shift during each iteration from the information contained in the resolved eigenvector. Therefore, excellent convergence is obtained. With the features of fast convergence and parallel processing, the proposed algorithm offers a feasible solution for high-throughput and real-time processing. In addition, compared to the SPM with super linear convergence, it also outperforms in complexity.

REFERENCES

[1] G. Lebrun, J. Gao, and M. Faulkner, “MIMO transmission

over a time-varying channel using SVD," IEEE Transactions on Wireless Communications, vol. 4, no. 2, pp. 757-764, 2005.

[2] C. H. Yang, C. W. Chou, C. S. Hsu, and C. E. Chen, "A systolic array based GTD processor with a parallel algorithm," IEEE Transactions on Circuits and Systems I: Regular papers, vol. 62, Iss. 4, pp. 1099-1108, Apr. 2015.

[3] Y. T. Huang, K. T. Chen, and C. K. Wu, "A high-throughput unified SVD/QRD precoder design for MIMO OFDM systems," in IEEE International Conference on Digital Signal Processing (DSP), 2015, pp. 1148-1151.

[4] C. H. Wu, C. Y. Liu, and P. Y. Tsai, " Design of an SVD engine for 8x8 MIMO precoding systems," IEEE International Symposium on Circuits and Systems, 2017, pp. 1-4.

[5] C. Z. Zhan, Y. L. Chen, and A. Y. Wu, "Iterative Superlinear-Convergence SVD Beamforming Algorithm and VLSI Architecture for MIMO-OFDM Systems," IEEE Transactions on Signal Processing, vol. 60, no. 6, pp. 3264-3277, June 2012.

[6] Junting Chen and Vincent K. N. Lau, "Multi-stream iterative SVD for massive MIMO communication systems under time-varying channels," 2014 IEEE International Conference on Acoustics, Speech and Signal Processing (ICASSP), 2014, pp. 3152-3156.

[7] P. Y.Tsai and C. Y. Liu, "Reduced-Complexity SVD with Adjustable Accuracy for Precoding in Large-scale MIMO Systems," IEEE Workshop on Signal Processing Systems (Sips), Nov. 2015, pp1-5.

[8] S. Jaeckel, L. Raschkowski, K. Börner, and L. Thiele, "QuaDRiGa: A 3-D Multi-Cell Channel Model With Time Evolution for Enabling Virtual Field Trials," IEEE Transactions on Antennas and Propagation, vol. 62, Iss. 6, pp. 3242-3256, Jun. 2014.

[9] 3GPP TR 36.873, v12.6.0, "Study on 3D channel model for LTE", Sep. 2017.

[10] O. E. Ayach, R. W. Heath, S. Abu-Surra, S. Rajagopal, and Z. Pi, "Low Complexity Precoding for Large Millimeter Wave MIMO Systems," in 2012 IEEE International Conference on Communications (ICC), Jun. 2012, pp. 3724–3729.

[11] K. N. Hsu, C. G. He, and Y. H. Huang, "Low-Complexity Hybrid Beam-Tracking Algorithms and Architectures for mmWave MIMO Systems," IEEE International Symposium on Circuits and Systems, 2016, pp. 1-4.

[12] M. T. Heath, Scientific Computing: An Introductory Survey, McGraw-Hill, 2005.